

LAP JOINT RESISTANCE OF Nb₃Sn CABLE
TERMINATION FOR THE ICCS-HFTF 12 TESLA
COIL PROGRAM

M.M. Steeves and M.O. Hoenig
M.I.T. Plasma Fusion Center
August 1982

PFC/RR-82-22

DOE/ET-51013-52
UC 20B

LAP JOINT RESISTANCE OF Nb₃Sn CABLE TERMINATIONS FOR
THE ICCS-HFTF 12 TESLA COIL PROGRAM*

BY

M.M. STEEVES AND M.O. HOENIG
M.I.T. PLASMA FUSION CENTER

ABSTRACT

Lap joint resistance as a function of current and magnetic field has been measured across prototypal 12 Tesla Coil conductor cable terminations. The terminations were at the ends of a 2.2 m Nb₃Sn hairpin of internally cooled and cabled superconductor (ICCS), and were soft soldered to NbTi bus bars. The resulting lap joints were each 15 cm long with a contact area of 19.8 cm². The maximum lap joint voltage drop was 75 μ V at 21 kA and 4.2 K, with the cable center at zero magnetic field. This represents an upper bound on all measured voltage drops, including those with the cable center at 10 and 12 T, and corresponds to a maximum heat flux of 0.01 w/cm². The results imply that the 12 Tesla Coil, with four lap joints, would dissipate less than 7 watts in the steady-state at 21 kA. The zero field results and results at cross fields of 10 and 12 T are discussed. Manufacturing and experimental parameters relevant to this study are also considered.

*Supported by U.S. D.O.E. Contract DE-AC02-78ET-51013

TABLE OF CONTENTS

	<u>PAGE</u>
1. INTRODUCTION.....	1
2. PURPOSE AND DESIGN CONSTRAINT.....	2
3. SUMMARY OF RESULTS.....	4
4. CONCLUSIONS.....	5
5. DESCRIPTION OF TEST CONDUCTOR.....	6
5.1 Test Hairpin.....	6
5.2 Wire Parameters.....	8
5.3 12 Tesla Program ICCS.....	11
5.4 Fabrication of Terminations.....	13
5.5 Superconductor Activation.....	13
5.6 Termination Lap Joints.....	15
6. EXPERIMENT.....	20
7. RESULTS.....	25
7.1 Lap Joint Voltage.....	25
7.2 Lap Joint Resistance.....	26
7.3 Lap Joint Power.....	27
7.4 Cable Short Sample Characteristic.....	31
7.5 Lap Joint Voltage Components.....	31
8. ANALYSIS.....	33
8.1 Transverse Resistance Model.....	33
8.2 Longitudinal Resistance Model.....	38
9. DISCUSSION.....	41
9.1 Cable Critical Current.....	41
9.2 Background Noise.....	42
9.3 Recommendations for Future Work.....	43
9.4 Significance of Experiment.....	44
10. ACKNOWLEDGMENT.....	45
11. NOMENCLATURE.....	45
12. REFERENCES.....	47

1. INTRODUCTION

Lap joint resistance as a function of current and magnetic field has been measured across prototypal 12 Tesla Coil conductor cable terminations. The terminations have been developed by MIT and Airco for use in the ICCS-HFTF 12 Tesla Coil, sponsored by the Department of Energy.^{1,2,3} This coil has been designed to test an internally cooled and cabled superconductor (ICCS) as a high field prototype for large coils in fusion engineering devices. The ICCS consists of cabled, multifilamentary niobium-tin superconductors encapsulated in a production-welded, vacuum-tight, stainless steel sheath. The sheath provides structural support for the cable and serves as a cryostat for forced cooling with supercritical helium. The cable provides large heat transfer surface area per unit length of superconductor and generates high helium turbulence even for small heat inputs, thus enhancing stability at minimal coolant velocity. The terminations provide electrical and hydraulic interfaces for connection to the ICCS. Electrical interfaces in the 12 Tesla Coil will be termination lap joints, and the purpose of this study was to evaluate the envisioned termination lap joints.

The termination lap joints connect the three 40 meter, series-connected, double pancakes of the 12 Tesla Coil. Overall coil performance will be evaluated by tests of transient and steady-state stability, scheduled at the High Field Test Facility (HFTF) of Lawrence Livermore National Laboratory in 1983. The 12 tesla conductor, although activated for high field operation, is geometrically identical to the conductor of the Westinghouse Large Coil Program (LCP).⁴ The soldered lap joint termination technology of the 12 Tesla Program complements the fusion-welded, butt joint termination technology the Westinghouse LCP.⁵ The technology of ICCS terminations is fundamental to the development

of cable-in-conduit conductors, and both lap and butt joint terminations are viable alternatives to a coil designer..

This report describes the fabrication, testing and performance of a 2.2 meter long ICCS, terminated at both ends, and bent into a hairpin to expose the cable center to an external magnetic field. Hairpin geometry, wire parameters and ICCS parameters are discussed. Termination fabrication, superconductor activation, and lap joint geometry are also considered. The methodology of the experiment and test results are presented and analyzed. Conclusions are drawn and recommendations for future work are presented.

2. PURPOSE AND DESIGN CONSTRAINT

2.1 Purpose

The purpose of this experiment was to evaluate the envisioned 12 Tesla Coil termination lap joints. More specifically, the experiment was to determine whether developmental joints of minimal length (15 cm) would carry design currents up to 20 kA at 4.2 K consistent with low heat generation and uniform current transfer across each joint.

2.2 Design Constraint

The 12 Tesla Coil lap joints are constrained by the physical size of the HFTF cryostat. The principal restriction involves joint length as shown in Fig. 1. Each joint must lie between the split-pair NbTi coils of the HFTF background field set, because there is not enough room for the joints to extend radially beyond the coil stack.

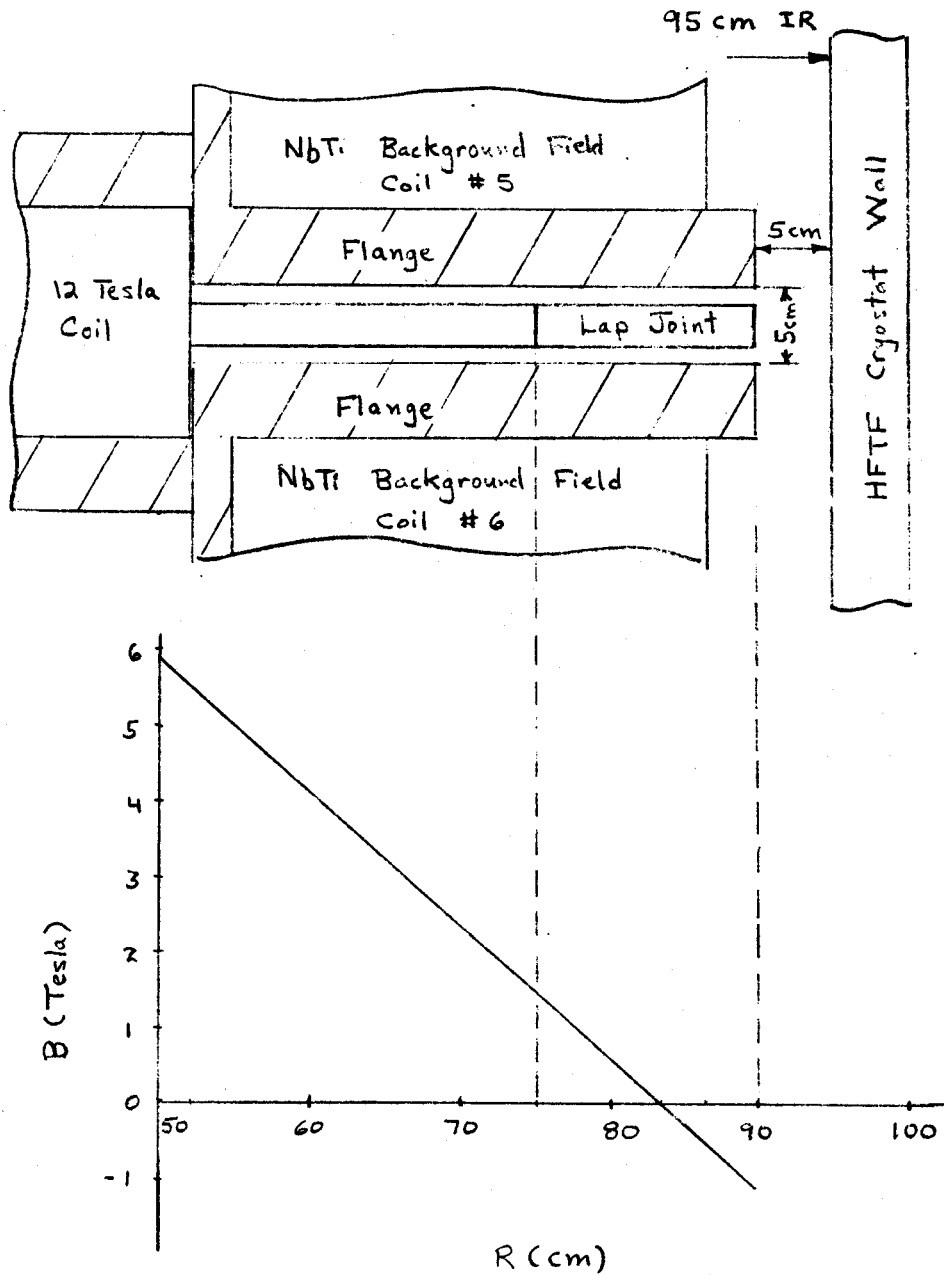


Figure 1. Relative position of the 12 Tesla Coil termination lap joints in the Livermore High Field Test Facility (HFTF). Coil lap joints are constrained to lie in a 5 cm gap between two stainless steel flanges. The approximate field profile at the lap joints is also shown. References 1 and 2 provide further detail on the 12 Tesla Coil experiment.

3. SUMMARY OF RESULTS

Three tests were performed on the termination hairpin at 4.2 K. Note that the hairpin cable was a "hybrid" with 33% pure copper strands uniformly distributed among 67% Nb₃Sn strands, to accommodate the available power supply. The test results are summarized below.

- 3.1 With the center of the hairpin at zero field, current was raised to determine the thermal limit of the termination lap joints. No limit was encountered at 20,900 amperes, the peak output of the power supply. Current was held at this level for 30 seconds and produced a stable lap joint voltage drop of 75 microvolts. This represents a heat load of 1.6 watts per termination, equivalent to a liquid helium boil-off rate of 2.3 liters per hour per termination.
- 3.2 With the center of the hairpin at 12 tesla, current was again raised to determine if the lap joint thermal limit would precede the cable critical current limit. No thermal limit was encountered at 13,700 amperes. At 10,000 amperes, the voltage drop across the cable center was zero. The corresponding maximum lap joint voltage drop was 21 microvolts. Between 10,000 and 13,700 amperes, the voltage drop across the cable center rose from zero to 120 microvolts (14 μ V/cm). The maximum lap joint voltage drop also rose from 21 to 38 microvolts. This represents a heat load of 0.5 watts per termination, approximately one third the heat load in case 3.1.
- 3.3 With the center of the hairpin at 10 tesla, current was again raised to determine if the lap joint thermal limit would precede the cable critical current limit. Again no thermal limit was reached. At 17,900 amperes, the cable center developed a normal voltage of 30 microvolts. The corresponding maximum lap joint voltage drop was 41 microvolts. This represents a heat load of 0.7 watts per termination, approximately one half the heat load in case 3.1.

4. CONCLUSIONS

The following conclusions have been drawn from this experiment.

- 4.1 The Nb₃Sn terminations developed for the 12 Tesla Coil are thermally stable for currents typical of the expected 12 T experiment. The maximum voltage drop across the termination lap joints was 75 μ V at 21 kA. This implies that the 12 Tesla Coil, with four lap joints, would dissipate less than 7 watts in the steady-state at 21 kA.
- 4.2 There was no significant difference in the resistive heat loads developed by the two types of lap joints studied in this experiment. (See Fig. 4 for lap joint geometries.)
- 4.3 As terminated in the test, the actual nonhybrid (all Nb₃Sn) 12 T ICCS could be expected to have a critical current of approximately 15,500 A. This number is based on an electric field criterion of 1.5 μ V/cm. The corresponding critical current density would be 225 A/mm².
- 4.4 There was a nonuniform current distribution in the test cable. As many as 33% of the available Nb₃Sn strands may have been underutilized, causing the cable to go normal at lower than expected current densities at 10 and 12 tesla. Whether this is due to lap joint surface contact area, termination design, or other factors is not known at this time. Further investigation is needed.
- 4.5 At currents typical of the 12 tesla experiment, current transfer resistance was comparable to solder layer resistance in the lap joints. Lapped surface contact area and conductor aspect ratio (all lapped conductors were square) were responsible for this condition.

4.6 The manufacturing technology used to build the terminations appears to be satisfactory. At the time of this writing, photomicrographs of termination cross-sections are unavailable, so the average condition of termination strands is unknown. However, based on observed performance, compaction to a 5% void fraction results in reasonably low termination resistance (less than $2 \text{ n}\Omega$). Low resistance implies good metallurgical bonding with acceptably low wire damage.

5. DESCRIPTION OF TEST CONDUCTOR

5.1 Test Hairpin

The test conductor was a 2.2 meter ICCS, tightly bent into the shape of a hairpin prior to activation of the Nb_3Sn for easy insertion into the bore of a Bitter solenoid. The cable was diluted with 33% copper wire to accommodate the available power supply. This dilution was accomplished by forming "hybrid" triplets of one copper and two Nb_3Sn wires. Table 1 outlines the twist schedule of the 486 strand test cable. Note that the twist pitch of the 3^4 subcable, the axial distance corresponding to one 360° twist, was taken as the termination lap joint length (15 cm). The significance of this length is discussed in Section 5.6.

TABLE 1

TWIST SCHEDULE OF 12 TESLA COIL CABLE⁶
(Identical to LCP Westinghouse)

<u>CABLE ELEMENT</u>	<u>TWIST PITCH</u>
1 (Single Strand)	2.5 cm* (1 in)
3 ¹ (Triplet)	2.5 cm (1 in)
3 ² (Triplet of Triplets)	3.8 cm (1.5 in)
3 ³	7.6 cm (3 in)
3 ⁴	15.2 cm (6 in)
6 x 3 ⁴	30.5 cm (1 ft)

* When triplets are made, individual strands are internally twisted on the same pitch as the triplet.

Figure 2 shows the termination test hairpin. The terminations were made by Airco Superconductors, Carteret, N.J., according to MIT specifications. The terminations were 23 and 33 cm long, to allow for study of the relationship of lap joint length to voltage drop, should 15 cm joints develop excessive voltage. The terminations were not solid in cross-section and had central Monel cooling tubes. With the 12 Tesla Coil, the cooling tubes would be connected to a supercritical helium bellows pump. With the test hairpin, the ends of the cooling tubes were left open, and the entire assembly was immersed and tested in pool-boiling liquid helium at 4.2 K.

Sections A-A, B-B and C-C illustrate the geometry of the termination, Monel tube, and ICCS. The shape changes between the three sections are a result of the way the terminations are made, as explained in Section 5.4. The central 64 cm was not encapsulated in stainless steel to allow the cable to be bent on a 5 cm radius. Two 1.6 mm wall stainless steel channels, not shown in Fig. 2, were used to mechanically support the hairpin throughout the experiment. The hairpin was placed between the channels prior to activation of the superconductor, and left undisturbed in this position after activation and during the experiment.

5.2 Wire Parameters

The multifilamentary niobium-tin wires, central to the 12 tesla cable and terminations, are described in Table 2. As reported by Airco, when activated for 30 hours at 750 C, these wires possess a noncopper critical current density of 300 A/mm^2 at 12 tesla, evaluated by an electric field criterion of $1.5 \text{ } \mu\text{V/cm}$.⁴ This translates into a critical current of 41 amperes per wire,

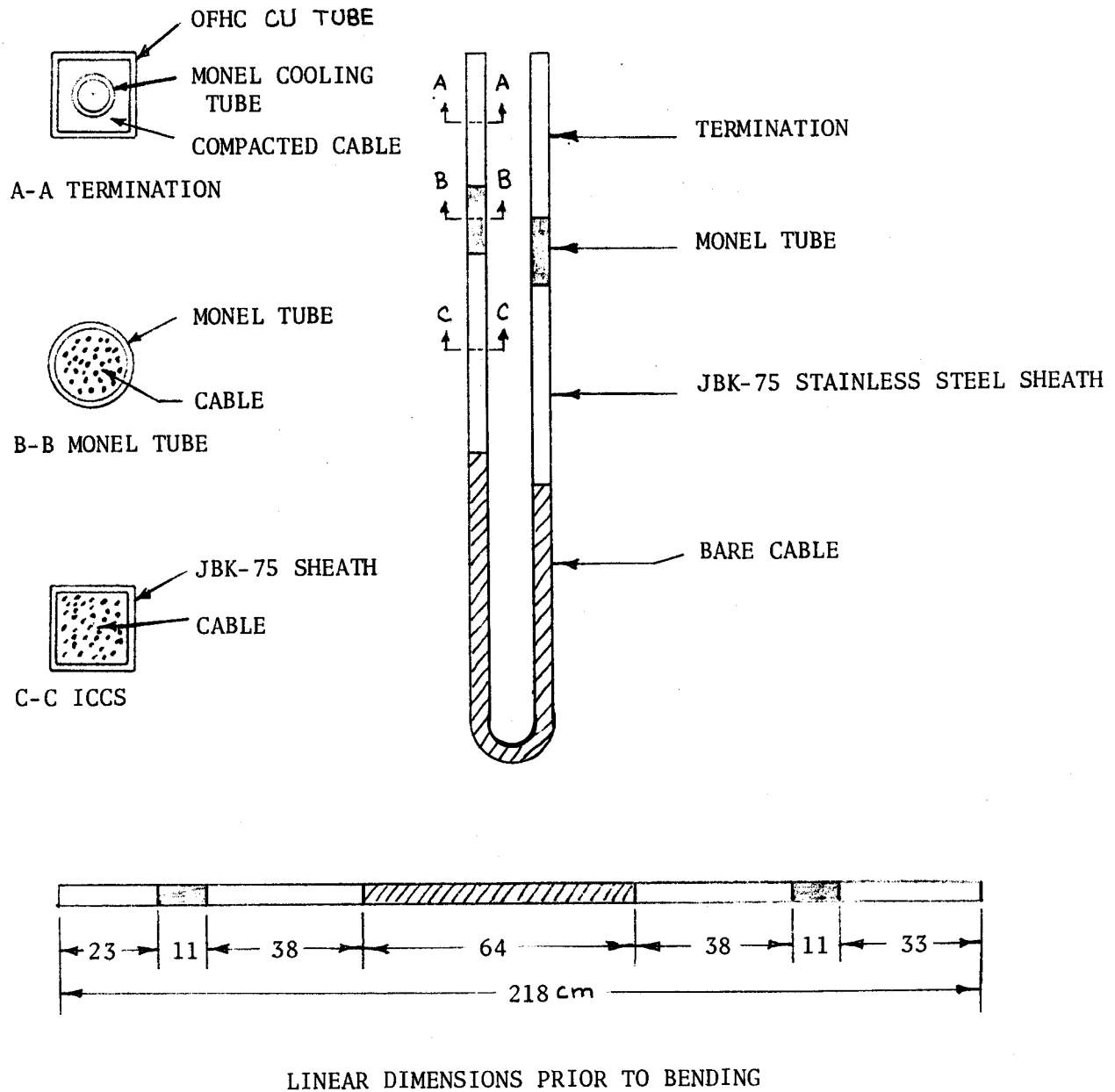


Figure 2. Termination test hairpin (dimensions in centimeters). Sections A-A, B-B and C-C show the change in ICCS geometry as one moves toward the cable center. The Monel tube was chosen for its weldability to both copper and stainless steel.

TABLE 2

PARAMETERS OF AIRCO MULTIFILAMENTARY Nb₃Sn
SINGLE STRAND WIRE

Diameter	0.7 mm
Copper-to-Noncopper Ratio	1.8/1
Matrix	Bronze
Niobium Filaments Per Strand	2869
Filament Diameter	3.5 μm
Weight Percent Tin	13%
Resistivity Ratio	50*
Surface Coating - Termination Test Hairpin	CuS ⁸
Surface Coating - 12 Tesla Coil Wire	Oil**

*Average of 8 samples, in batches of 1 and 7, fired separately for 30 hours at 750°C. Three wires from batch 7 were oil coated.⁷

**Near-A-Lard #250-H Oil (Drawing Lubricant).

and scales to 13,300 amperes per 486 strand hybrid cable, assuming no degradation in current carrying capacity due to cabling and compaction. Single wire measurements of critical current at MIT show the Airco results to be conservative (about 20% below our measurements).

The wires used in the termination test hairpin were coated with a nominal 4 μm layer of copper sulfide insulation. This coating was chemically removed from the termination lengths, but not removed from the remaining length of cable. The presence of copper sulfide strand insulation meant that any current transfer between strands took place in the terminations and not in the body of the cable. Current flow and power dissipation in the terminations were therefore influenced by the presence of the sulfide strand insulation. This aspect of the experiment did not simulate the final form of the 12 Tesla Coil. However, the sulfide coating effectively prevented any current sharing between strands in the body of the cable. The sulfide coating, therefore, produced a more conservative test of the termination lap joints.

5.3 12 Tesla Program ICCS

The ICCS of the 12 Tesla Program is geometrically identical to that of the Westinghouse Large Coil Program.⁵ Parameters of this conductor are listed in Table 3, and the conductor can be described as a cable-in-pipe conductor designed for cooling with supercritical helium.⁹

TABLE 3

12 TESLA PROGRAM ICCS

Outside Dimensions	2.08 x 2.08 cm
Outside Corner Radius	0.46 cm
Final Wall Thickness	0.17 cm
Sheath Material	JBK-75 Super Alloy SS
Void Fraction	35%
Cable Configuration	6 x 3 ⁴

5.4 Fabrication of Terminations

Airco superconductors, manufacturer of the terminations for the 12 Tesla Coil lap joints, used the following steps in their production. First, short lengths of sheath were removed from both ends of the test conductor by grinding a slot in the sheath and wedging the sheath apart. The stainless steel foil around the cable was cut away, and the exposed cable was acid cleaned and rinsed to provide low resistance bonding between adjacent strands. An OFHC copper tube was slid over the exposed cable and onto the undisturbed steel sheath adjacent to the cable. Then the 3⁴ subcables were spread open and a Monel cooling tube inserted along the cable center. The subcables were closed around the cooling tube, and the OFHC copper tube was pulled back over the cable. At this point, a short Monel tube was slid over the copper tube and TIG welded to both the copper and stainless steel. (With future terminations, the copper tube will be welded directly to the stainless steel.) The copper tube was then swaged to approximately 5% void and squared-off in a Turk's head, completing fabrication. Figure 3 summarizes the steps in making 12 Tesla Coil terminations.

5.5 Superconductor Activation

The Nb₃Sn superconductor was activated by baking the test hairpin in a tube furnace for 30 hours at 750C. Prior to activation, the hairpin was secured between two stainless steel channels (Type 304). These channels served both as a firing fixture and as a test fixture and were designed to protect the hairpin from damage during handling and testing, since strains greater than 0.2% are damaging to Nb₃Sn. After activation, the hairpin was never removed from the channels and was insulated from the channels by G-10 shims.

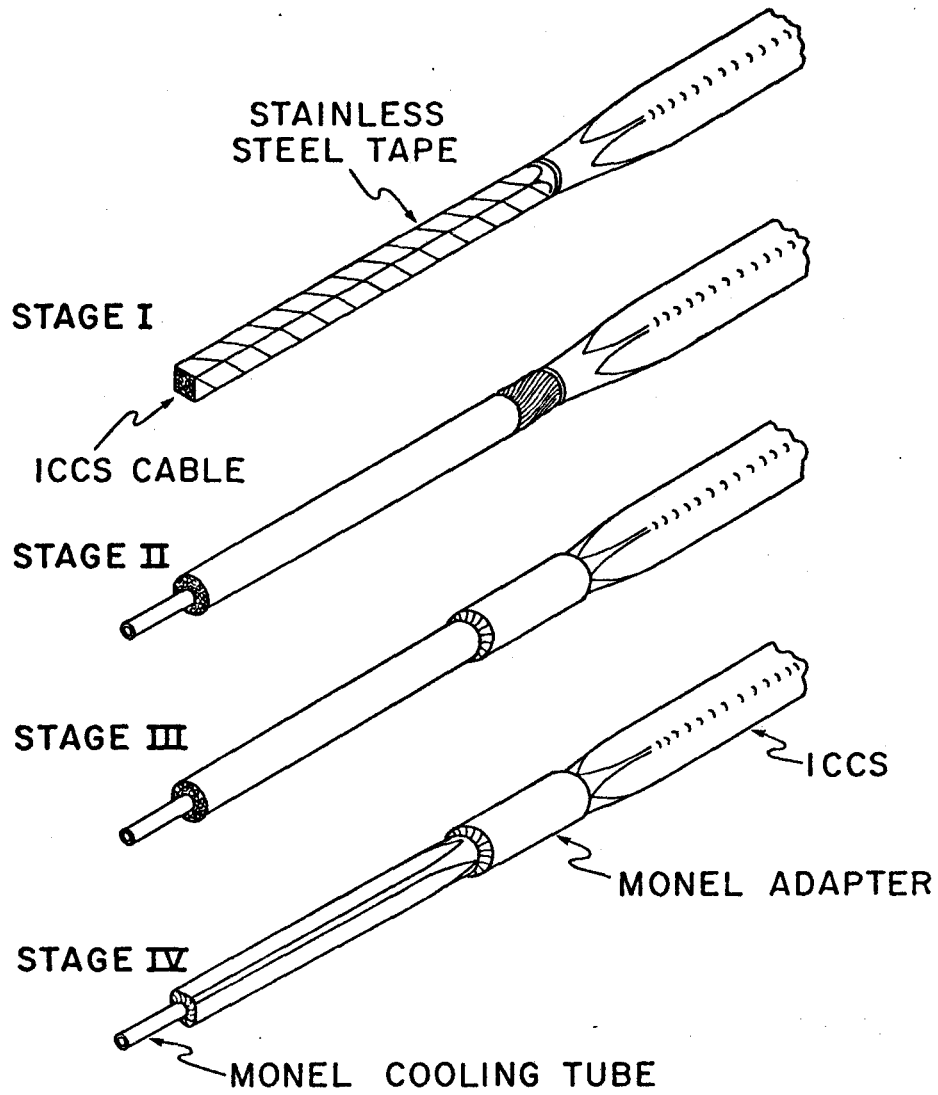


Figure 3. Stages in the fabrication of ICCS terminations for the 12 T program.

The hairpin was activated inside a clean quartz tube in a dry helium atmosphere. The quartz tube fit into the bore of the tube furnace and had an end flange equipped with gas and thermocouple ports. The temperature profile in the furnace was monitored with thermocouple probes during activation.

5.6 Termination Lap Joints

Lap joints were made between the Nb₃Sn terminations and short lengths of NbTi Mirror Fusion Test Facility conductor core. Table 4, taken from reference 10, lists MFTF conductor core parameters.

TABLE 4

MFTF MAGNET CONDUCTOR CORE PARAMETERS

(See Reference 10)

Critical Current (NbTi)	10 kA @ 7.5 T, 4.2 K
Copper-to-Superconductor Ratio	1.7/1
Number of Filaments	480
Filament Diameter	0.20 mm
Twist Pitch	180 mm
Conductor Resistance Ratio	150/1
Size	6.5 x 6.5 mm

The joints were made by lapping the pretinned terminations and MFTF cores and soft soldering with 60/40 (Sn/Pb) solder with an activated rosin flux core. Prior to joining, the pretinned surfaces were lightly coated with zinc chloride solder paste to dissolve oxides and prevent further oxidation. The lapped joints were tightly clamped while soldering took place. Two parallel MFTF conductor cores were soldered to one face of each termination as shown in figure 4. The other three faces of the termination were left open.

Although one termination measured 23 cm, and the other 33 cm, the two lap joints were 15 cm each. Short 15 cm lap joints reflect space constraints imposed on the 12 Tesla Coil by the HFTF 2 m diameter cryostat. As mentioned previously, lap joints between subcoils are radial, and long lap joints would prevent the 12 Tesla Coil from fitting into the HFTF cryostat.

The two lap joints were not identical with respect to overall current direction or internal current distribution. In one case, current entered and exited the same side of the joint, while in the other case, current entered one side and exited from the other. The two styles of joint are here called "praying hands" and "clasping hands". In this context, the word hand means one of the two lapped conductors. Praying hands implies that the palms are together, one hand a mirror image of the other. Thus in a praying hands lap joint, current would enter one conductor, cross the interface, reverse direction and exit the other conductor. Clasping hands implies that the palms are placed together as in a hand shake. Current does not change direction in a clasping hands lap joint. The two configurations were tested because the 12 Tesla Coil will have two praying hands lap joints connecting

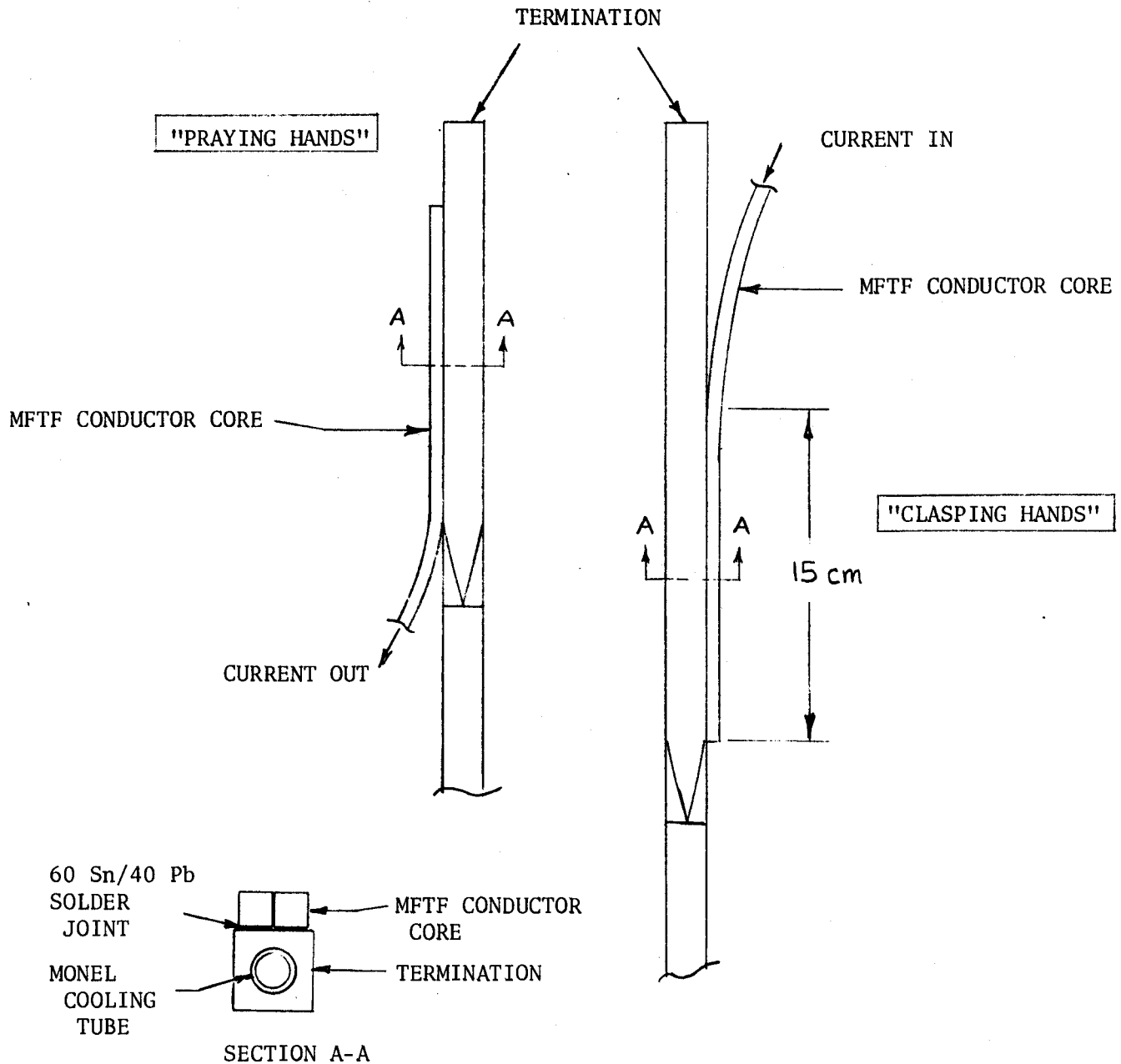


Figure 4. Termination test lap joints. The joints are called "praying hands" and "clasping hands" to denote their relative geometries. MFTF conductor cores (NbTi) were soft soldered to one surface of each termination as shown.

the three double pancakes, and two clasping hands lap joints connecting the two coil terminals.

The 15 cm length of lap joint corresponds to the twist pitch of the six 3^4 subcables (81 strands each). In one 15 cm twist pitch, each strand occupies every cross-sectional position in the subcable. Hence in one twist pitch, each strand comes in solid contact with the OFHC swage tube surrounding the entire cable in the termination region. However, in one subcable twist pitch, each strand does not occupy every cross-sectional position in the termination.

The termination was square in cross-section. In one subcable twist pitch, all strands touched at least one of the four sides of the squared-off OFHC copper swage tube, but no strand touched all four sides. This meant that a 15 cm lap joint on one of the four possible surfaces favored some Nb₃Sn strands over others. If current transfer resistance is defined to be the sum of surface copper resistance and composite region (filaments, matrix and copper) resistance, then strands adjacent to the lap joint surface had lower current transfer resistance than those not adjacent to the lap joint surface.¹¹ This implies that 15 cm lap joints to one surface of the termination should represent a worst case in terms of power dissipation. Conversely, 15 centimeter lap joints on all four surfaces should represent a best case in terms of power dissipation. Figure 5 illustrates how some subcables are favored over others by the arbitrary selection of one out of four possible lap joint surfaces.

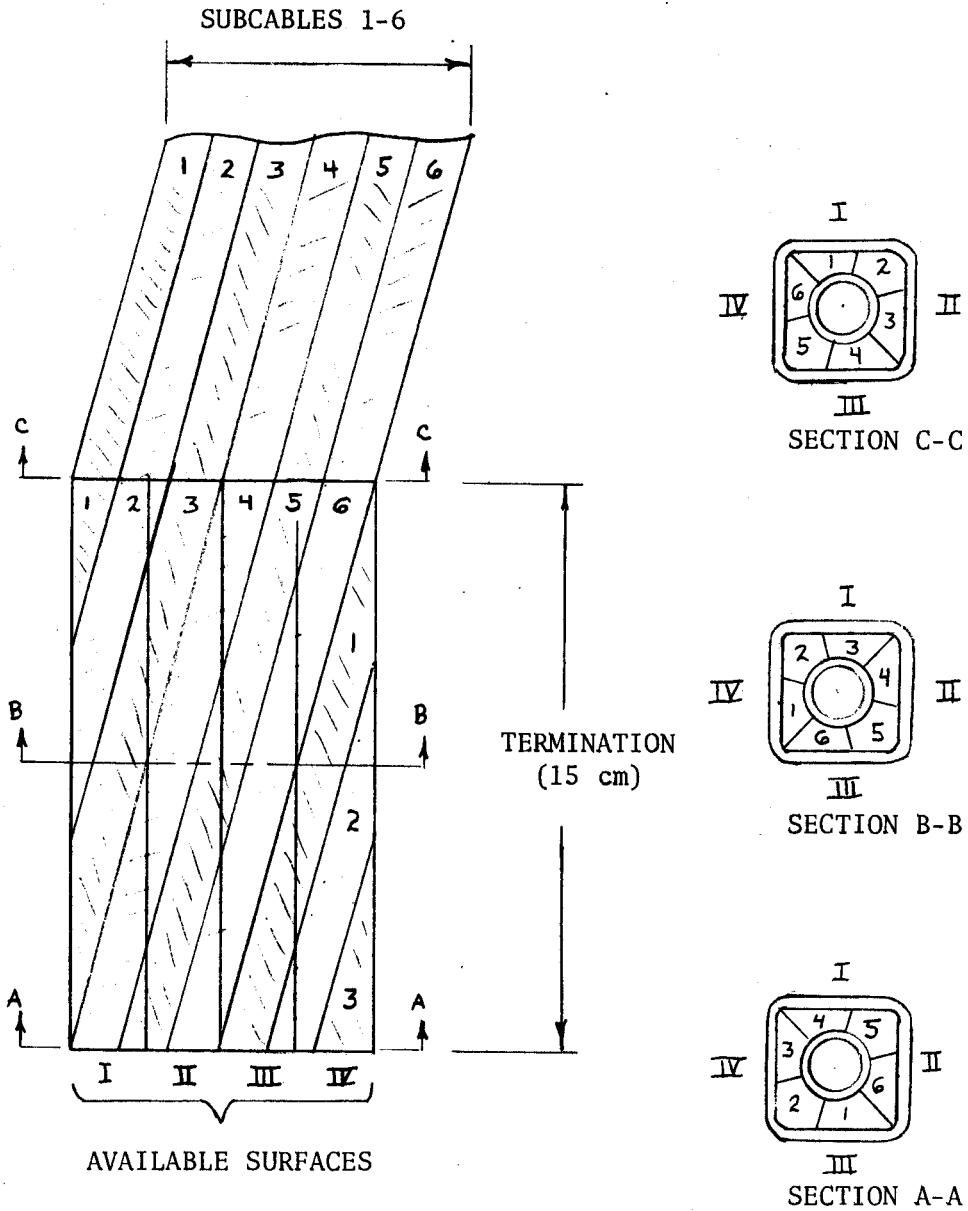


Figure 5. Four termination surfaces available for lap joints. Surface I presents lower current transfer resistance to subcables 1-4. A right hand rotation of subcables is shown.

6. EXPERIMENT

The termination experiment simulated 12 Tesla Coil operating conditions with worst case lap joints. Independent variables, other than lap joint geometry, were current and background magnetic field at the center of the hairpin cable. Dependent variables were voltages measured at the lap joints and across the hairpin cable.

The test hairpin was subject to Lorentz force from the background magnetic field of the Bitter solenoid. A force-compensating hairpin of copper and MFTF conductor was built and placed back-to-back to the test hairpin to react the Lorentz forces (approximately 3000 pounds at 12 tesla). The test hairpin and backing hairpin were electrically connected in series as shown in figure 6.

Voltage taps were placed across the termination lap joints and across both hairpins. The lap joint signals were amplified, filtered, sampled and stored in a Biomation waveform recorder (Gould Co.). The stored signals were then plotted with X-Y recorders to provide permanent records. A nano-volt reference source was used to calibrate all channels by providing known input voltages which were amplified, filtered, sampled and stored and then plotted in a manner identical to the experimental voltages.

Voltage taps were soldered to the lap joints as shown in figure 6. The taps were placed across the axial lengths of both the terminations and MFTF conductors. This arrangement was chosen to partition the lap joint voltages, if possible, and to provide measurement redundancy. Voltage taps on the clasping hands lap joint were numbered 1-4, with tap 1 taken as reference. Taps on the

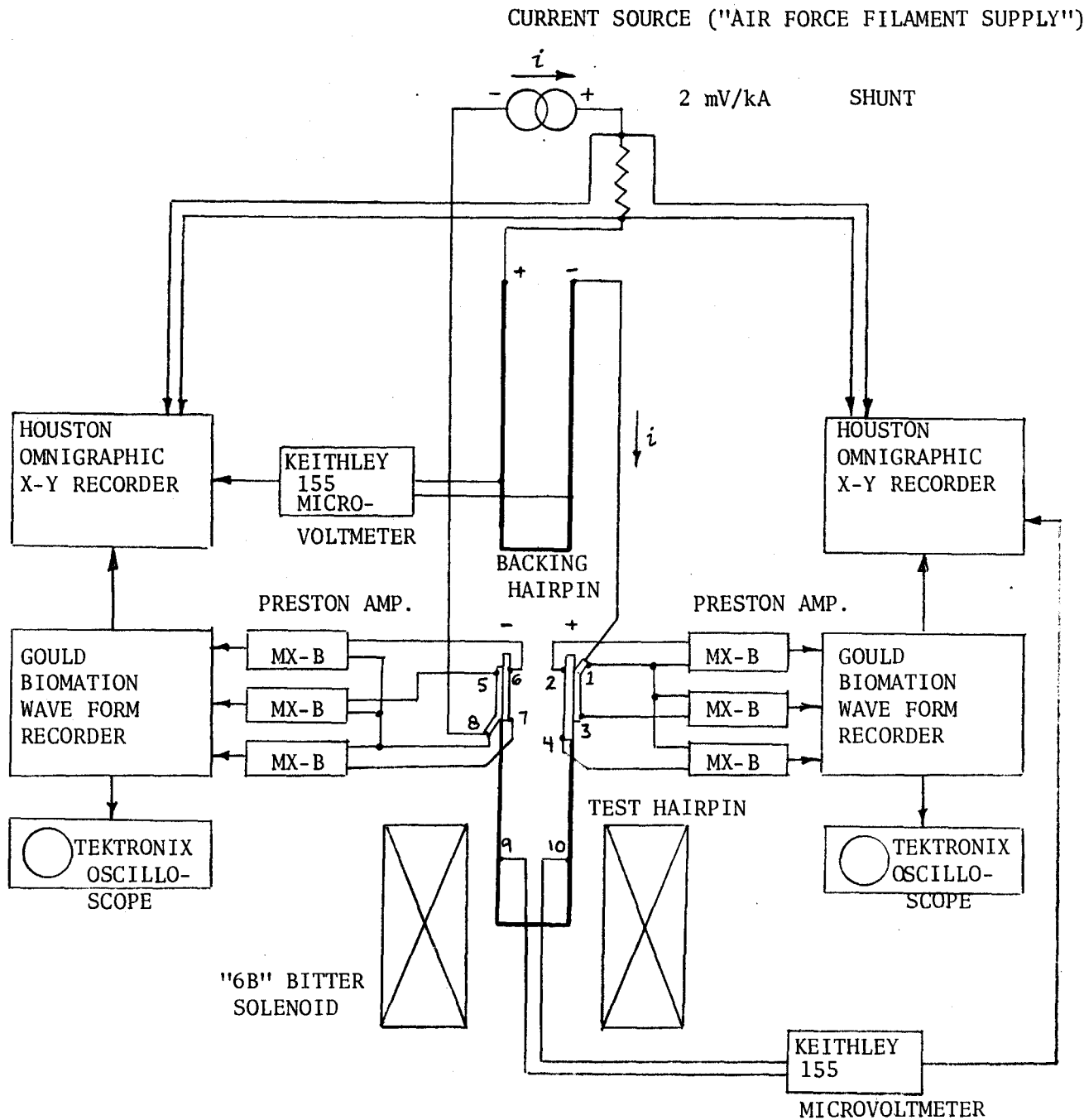


Figure 6. Termination test experimental arrangement. Three voltage drops were measured across each lap joint and one measured across the cable center. Voltage taps are numbered 1-10.

praying hands lap joint were numbered 5-8, with tap 8 taken as reference.

Listed below are measured lap joint voltages.

Long (33 cm) termination, clasping hands lap joint:

$$v_{21} = v_2 - v_1 \quad (1)$$

$$v_{31} = v_3 - v_1 \quad (2)$$

$$v_{41} = v_4 - v_1 \quad (3)$$

Short (23 cm) termination, praying hands lap joint:

$$v_{58} = v_5 - v_8 \quad (4)$$

$$v_{68} = v_6 - v_8 \quad (5)$$

$$v_{78} = v_7 - v_8 \quad (6)$$

The experiment began with a continuous current ramp to 500 A with no background magnetic field. After about one minute at this current level, the test was stopped, voltage traces on the two oscilloscopes were checked to be sure that tap voltages were within acceptable limits, and the experimental arrangement was scrutinized. When inspection revealed no obvious problems, the test was continued by ramping the current at a rate of 300 A/sec to 15,500 A, where it was held for approximately 40 seconds. Although this was 1000 A above the 14,000 A rating of the vapor-cooled leads, no effects of overheating were observed.

After reducing the current to zero, the current was again ramped at 300 A/sec to 10,500 A. Then, in three steps, it was taken up to 20,900 A

(the limit of the power supply) where it was held for approximately 30 seconds at zero magnetic field. There was evidence of lead overheating on the X-Y plot of current (expanded "X4" scale) that was not immediately obvious on the oscilloscope trace (non-expanded "X1" scale). However, the termination test lap joints performed well with all measured voltages less than or equal to 75 μV .

At this point, the background magnetic field was turned on and raised to 12 tesla. The test current was raised in a series of steps to 13,600 A, where it was held for 22 seconds. A steady voltage of 120 μV was observed across the test hairpin, while lap joint voltages measured less than 40 μV . There was no evidence of lead overheating.

The background field was then lowered to 10 tesla and the current raised in a series of steps to 17,900 A, at which it was held for 72 seconds. At this point the two positive-polarity, vapor-cooled leads burned out. During the 72 second interval, a steady voltage of 30 μV was measured across the hairpin, while lap joint voltages measured less than 42 μV .

Figure 7 shows current as a function of time for the various test runs.

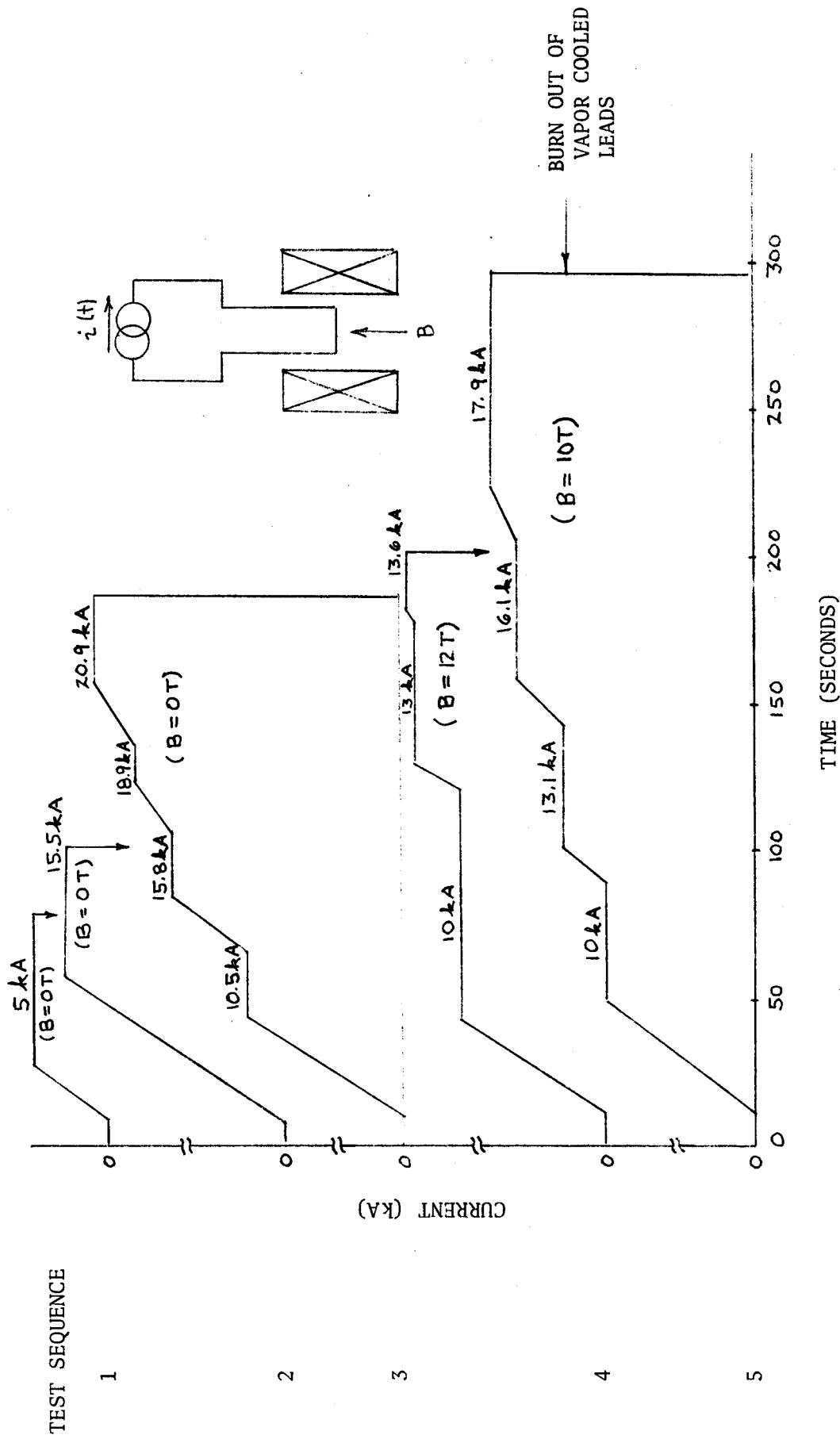


Figure 7. Termination test current-versus-time profiles. The test sequence starts at the top of the figure. Magnetic fields at the cable center are shown in parentheses.

7. RESULTS

7.1 Lap Joint Voltage

Table 5 lists maximum lap joint voltage drop as a function of test current and magnetic field at the cable center. Test current was limited to the maximum output of the power supply (20,900 A). The maximum voltage drops have the highest certainty of measurement and serve as upper bounds on all lap joint voltage data. Figures 8-10 show other data for the three runs listed below.

TABLE 5
MAXIMUM VOLTAGE DROP AS A FUNCTION OF CURRENT AND MAGNETIC FIELD

RUN NUMBER	MAGNETIC FIELD	TEST CURRENT	CLASPING HANDS CONFIGURATION, VT1-4	PRAYING HANDS CONFIGURATION, VT7-8
3	0T	20.9 kA	56 μ V (\pm 20 μ V)	75 μ V (\pm 20 μ V)
4	12*	13.6	38 (\pm 20)	33 (\pm 20)
5	10**	17.9	41 (\pm 20)	29 (\pm 20)

* Field at terminations approximately 500 Gauss.

** Field at terminations approximately 400 Gauss.

7.2 Lap Joint Resistance

Resistance and resistance-area product of the two lap joints have been calculated for the values listed in Table 5. The results show resistances to be highest in the high field and high current cases (Runs 3 and 4).

TABLE 6
LAP JOINT RESISTANCE AND RESISTANCE-AREA PRODUCT
(Joint Contact Area of 19.8 cm²)

RUN NUMBER	MAGNETIC FIELD	TEST CURRENT	CLASPING HANDS CONFIGURATION, VT1-4		PRAYING HANDS CONFIGURATION, VT7-8	
			JOINT RESISTANCE	RA	JOINT RESISTANCE	RA
3	OT	20.9 kA	2.7 nΩ	53 nΩ·cm ²	3.6 nΩ	71 nΩ·cm ²
4	12*	13.6	2.8	55	2.4	48
5	10**	17.9	2.3	46	1.6	32

* Field at terminations approximately 500 Gauss.

** Field at terminations approximately 400 Gauss.

As a note of clarification, the resistance area product allows one to separate the surface resistivity of the joint interface from the bulk resistivity of the copper. See Equation 7, page 33.

7.3 Lap Joint Power

Table 7 summarizes lap joint power and surface heat flux as a function of test current and magnetic field at the cable center. It implies that the 12 Tesla Coil, with four lap joints, would dissipate less than 7 watts in the steady-state at 21 kA.

TABLE 7

LAP JOINT POWER AND SURFACE HEAT FLUX
(Cooled Surface Area of 144 cm²)

RUN NUMBER	MAGNETIC FIELD	TEST CURRENT	CLASPING HANDS CONFIGURATION, VT1-4		PRAYING HANDS CONFIGURATION, VT7-8	
			POWER	HEAT FLUX	POWER	HEAT FLUX
3	0T	20.9 kA	1.17 w	0.008 $\frac{w}{cm^2}$	1.57 w	0.011 $\frac{w}{cm^2}$
4	12*	13.6	0.52	0.004	0.45	0.003
5	10**	17.9	0.73	0.005	0.52	0.004

* Field at terminations approximately 500 Gauss.

** Field at terminations approximately 400 Gauss.

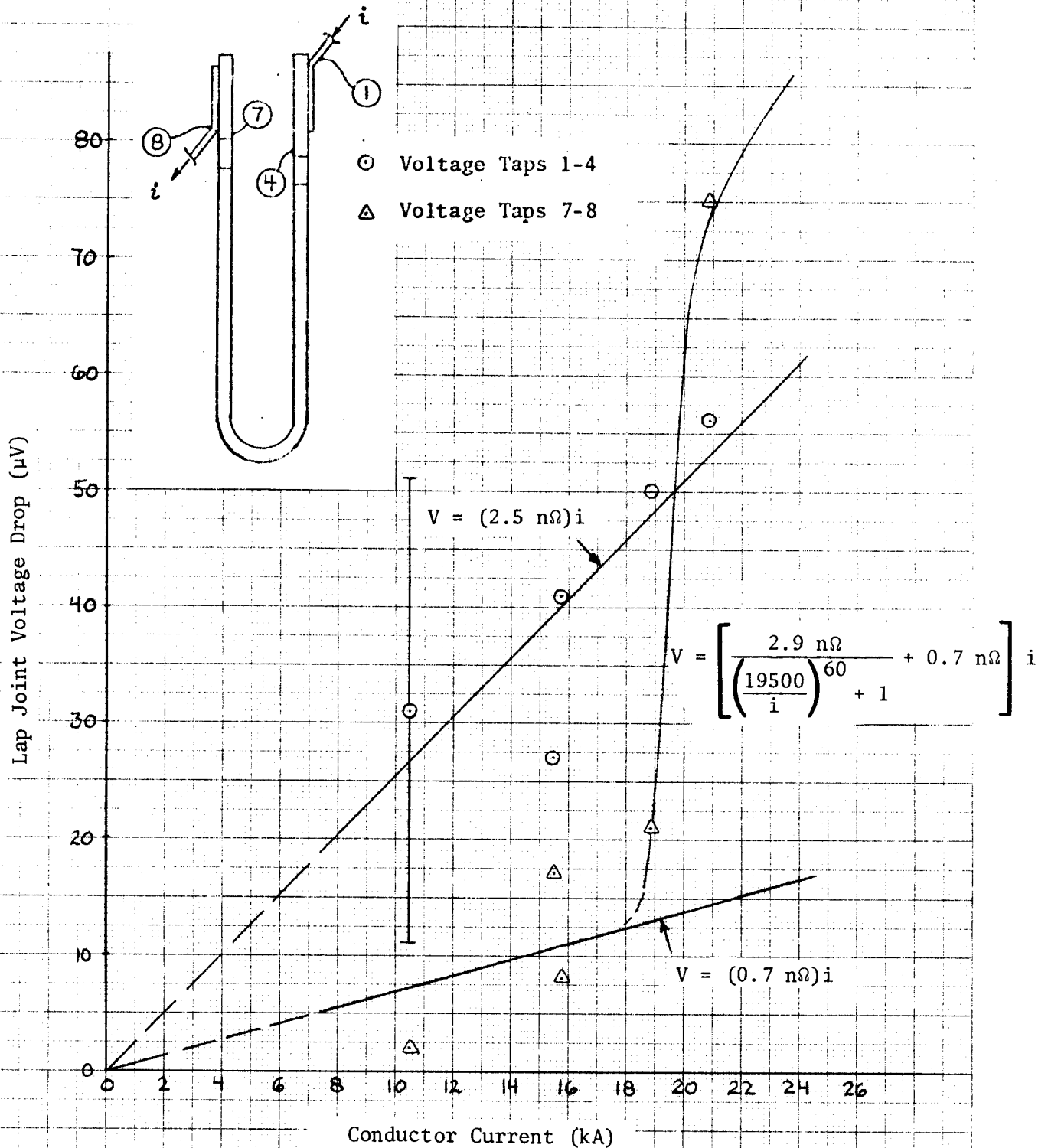


Figure 8. Lap joint voltage drop as a function of current at 4.2 K with no external magnetic field. Measurement uncertainty was $\pm 20 \mu\text{V}$. The praying hands lap joint (VT 7-8) appeared to have a nonlinear resistance. This could be due to measurement uncertainty or possibly longitudinal resistance in the lapped superconductors.

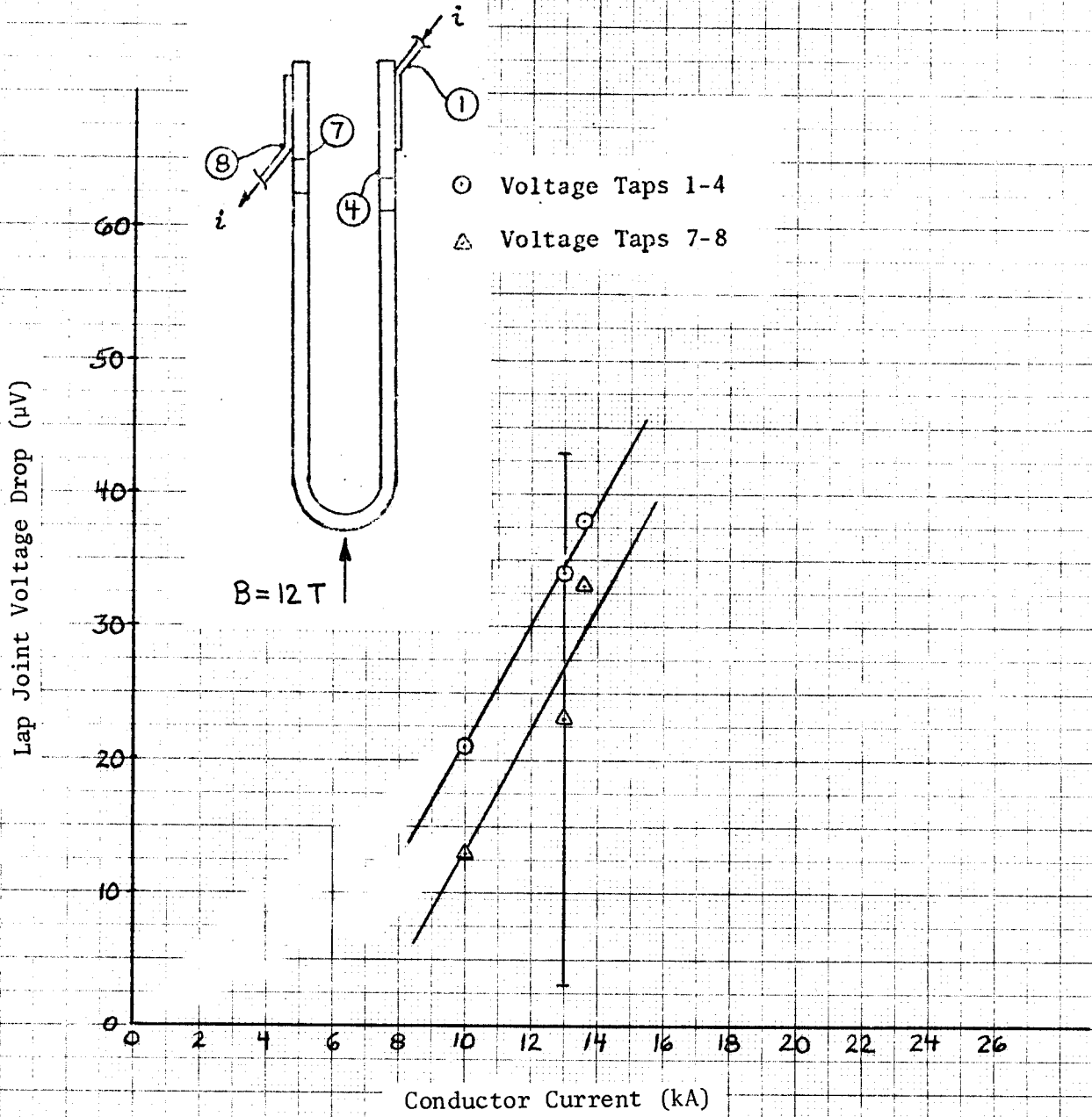


Figure 9. Lap joint voltage drop as a function of current at 4.2 K with the cable center at 12 T. Measurement uncertainty was $\pm 20 \mu\text{V}$.

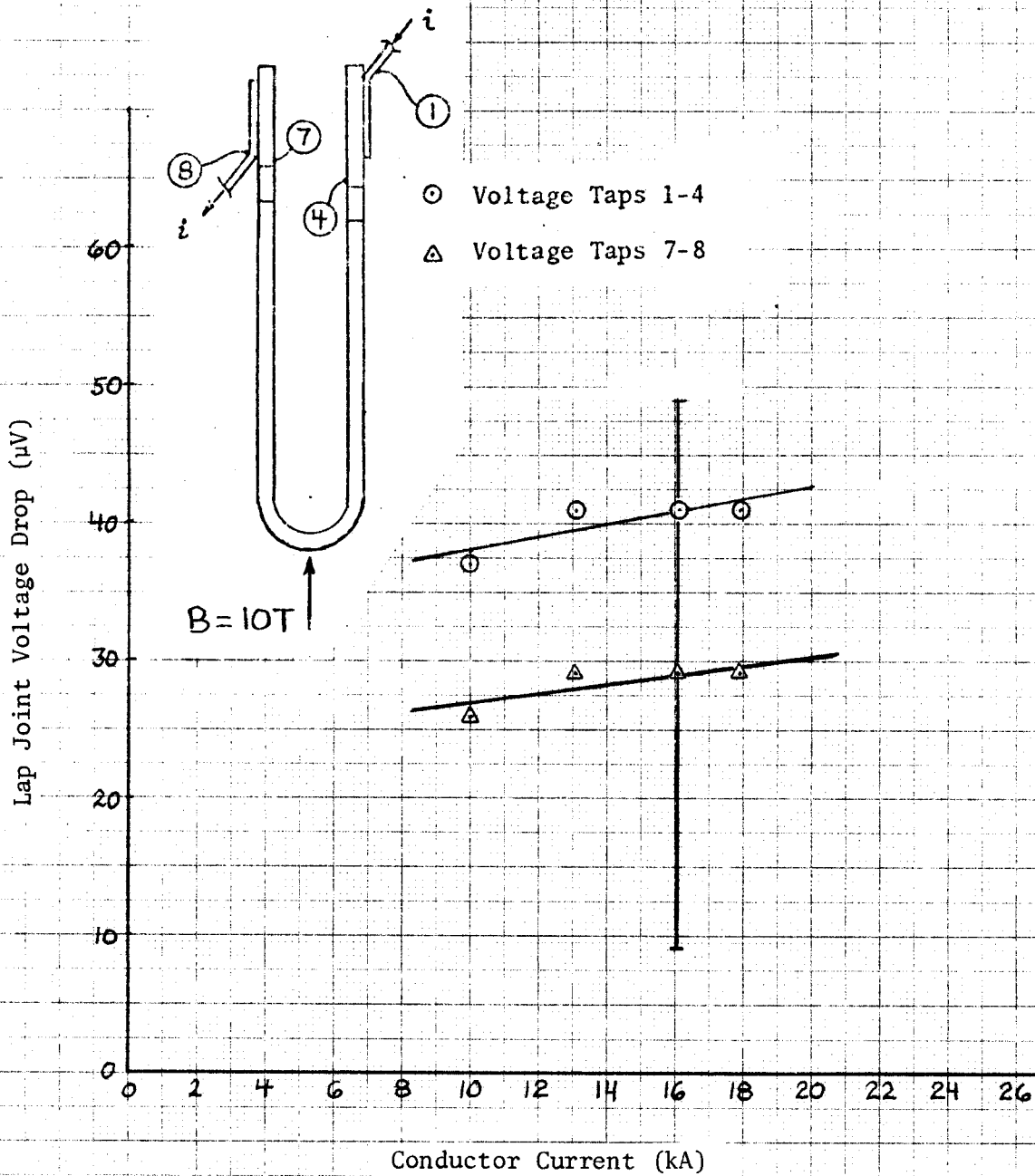


Figure 10. Lap joint voltage drop as a function of current at 4.2 K with the cable center at 10 T. Measurement uncertainty was $\pm 20 \mu V$.

7.4 Cable Short Sample Characteristic

The short sample characteristic of the hybrid cable (324 Nb₃Sn strands, 162 copper strands) is shown in Figure 11. Also shown are single wire measurements taken at MIT.¹² At 12 tesla, the hybrid cable had a critical current that was 59% of the current measured for single wires. Note that critical current data were evaluated by an electric field criterion of 1.5 μV/cm. The length of cable perpendicular to the Bitter coil magnetic field was taken as the centerline-to-centerline distance between vertical legs of the hairpin (8.7 cm).

7.5 Lap Joint Voltage Components

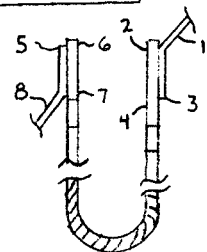
Table 8 lists voltage components associated with each lap joint voltage drop. These components indicate the electric field distribution in the joints. The apparent inconsistencies probably come from measurement uncertainty (± 20 μV).

TABLE 8
VOLTAGE COMPONENTS ASSOCIATED WITH MAXIMUM
LAP JOINT VOLTAGE DROPS

MAGNETIC FIELD	TEST CURRENT	v ₁₄	v ₁₂	v ₁₃	v ₂₄
OT	20.9 kA	56 μV	56 μV	53 μV	0 μV
12*	13.6	38	-	18	-
10**	17.9	41	29	23	12
MAGNETIC FIELD	TEST CURRENT	v ₇₈	v ₆₈	v ₅₈	v ₇₆
OT	20.9 kA	75 μV	44 μV	34 μV	31 μV
12*	13.6	33	10	11	23
10**	17.9	29	17	11	12

* Field at terminations approximately 500 Gauss.

** Field at terminations approximately 400 Gauss.



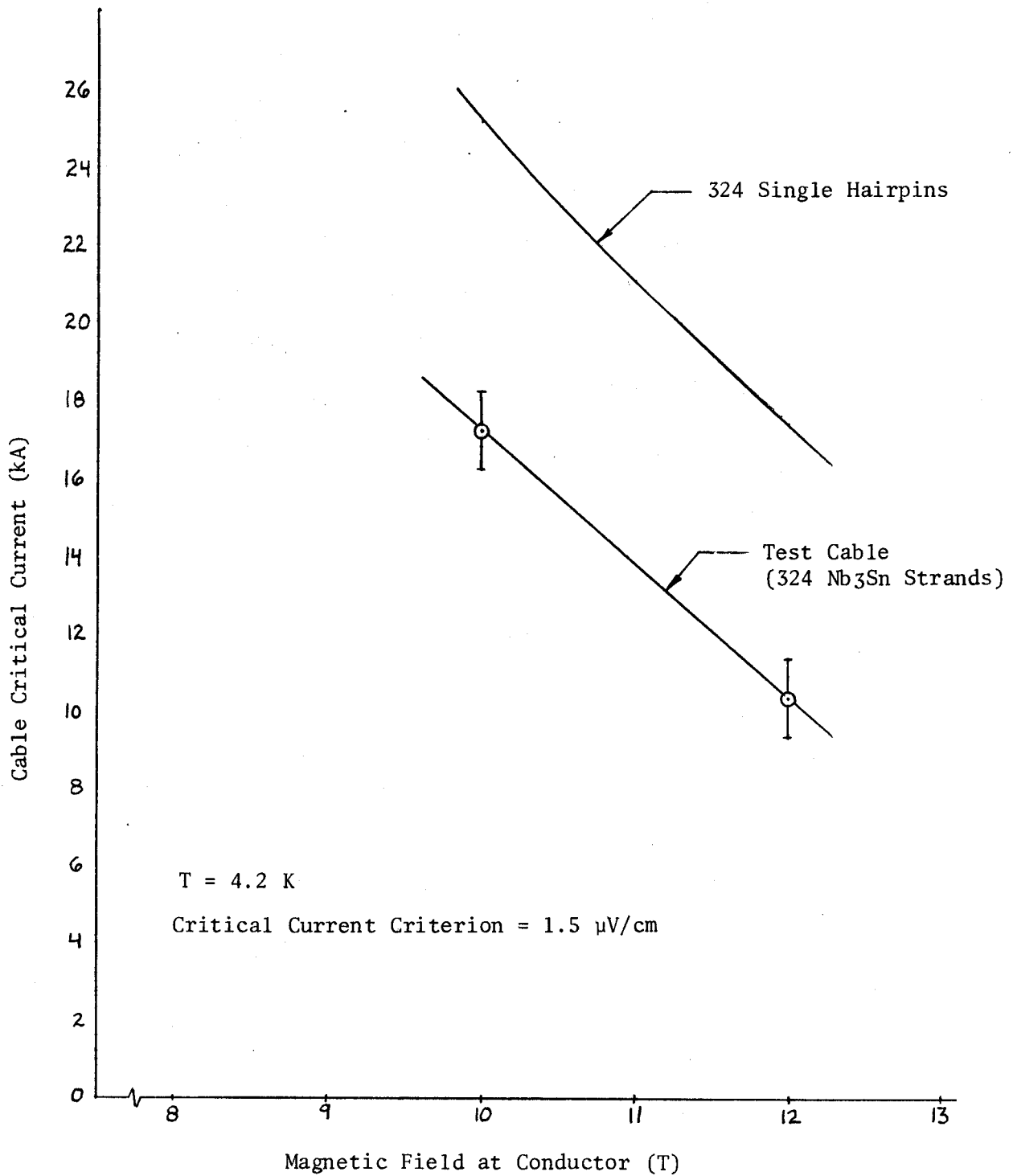


Figure 11. Performance of termination test cable relative to single wires. All conductors were reacted at 750 C for 30 hours. Cable strands were coated with copper sulfide; single strands were not.

8. ANALYSIS

The analysis of a lap joint between two conductors with embedded superconducting filaments is complicated by the anisotropic nature of the conducting medium. In some respects, the lap joint problem resembles that associated with current transfer lengths¹³, although the solder interface between the lapped conductors plays a major role in the behavior of the joint.

8.1 Transverse Resistance Model

In this model all voltage across the joint is assumed to be due to transverse current flow between the lapped conductors. Any longitudinal resistance is conveniently ignored, resulting in a straightforward and reasonably accurate model.

It should be noted that an ICCS termination can be plagued by a multitude of internal contact resistances, if metallurgical bonds between the wire strands themselves and between the strands and copper swage tube are not established. In the analysis which follows, complete metallurgical bonding is assumed, although this, of course, is not the case.

The analysis begins by dividing joint resistance into two components that can be classified as interface (solder and contact) resistance and current transfer (copper) resistance.¹¹ The components can be separated by writing the product of contact area and resistance as

$$A_j R_j = \rho_s + \rho_m t \quad (7)$$

(solder and contact term) (current transfer term)

where ρ_s is surface resistivity, ρ_m is matrix (or stabilizer) resistivity, and t is conductor thickness. This expression is conservative in assuming that the current transfer path is twice the half thickness of each conductor. At low currents, filaments closest to the interface carry most of the current, thereby shortening the current transfer length below t .

The $\rho_m t$ term assumes identical conductors on either side of the joint. In the case of the termination test lap joints, the two conductors were different, and this term may be rewritten as

$$\rho_m t = \frac{\rho_1 t_1}{2} + \frac{\rho_2 t_2}{2} \quad (8)$$

where ρ_1 and ρ_2 are the matrix resistivities of conductors 1 and 2, and t_1 and t_2 are their thicknesses.

Combining (7) and (8) and solving for maximum joint resistance yields

$$R_j = \frac{\rho_s + \frac{\rho_1 t_1}{2} + \frac{\rho_2 t_2}{2}}{A_j} \quad (9)$$

This expression has been used to estimate termination test lap joint resistances, bearing in mind that the resistivities given in (9) are somewhat uncertain.

The surface resistivity can be estimated from measurements reported in the literature.^{11,14,15} Table 8 lists some of the reported values for solders similar to the one used in this test.

TABLE 8
CONTACT SURFACE RESISTIVITY, SOLDER-COPPER INTERFACE

<u>DATA SOURCE</u>	<u>SURFACE RESISTIVITY</u> (4.2 K)	<u>MAGNETIC FIELD</u>
Hatch ¹⁴ - 50/50 solder (0.1 mm thick x 1.11 cm ²)	15 nΩ·cm ²	0T
Magnetic Engineering Association (per Hatch) - 50/50	50	0
Argonne National Laboratory (per Hatch) - 50/50	10	0
Goodrich ¹¹ - 63 Sn/37Pb	4.5	0-8 T
Rackov ¹⁵ - 50/50	10.6	7 T

As evident in Table 8, surface resistivity measurements vary by as much as an order of magnitude, although the distribution in reported resistivities is skewed toward a value of $10 \text{ n}\Omega \cdot \text{cm}^2$. The dependence of surface resistivity on applied magnetic field is somewhat ambiguous. For a 0.1 mm thick solder layer, reference 14 reports a factor of 2-3 increase in resistivity in going from 0 to 8 tesla. Reference 11 on the other hand, implies that surface resistivity is only weakly dependent on applied magnetic field.

Figure 12 shows lap joint resistance as a function of contact surface resistivity, with the resistivity ratio of the termination copper as a parameter. Also shown is a horizontal line corresponding to a resistance of $3.6 \text{ n}\Omega$ (See Table 6). This line is an upper bound on all test data, regardless of field. Assuming the surface resistivity to equal $10 \text{ n}\Omega \cdot \text{cm}^2$ and the resistance ratio of the MFTF conductor core to be 150 (See Table 4), one concludes that the apparent RRR of the termination copper is greater than 25. The measured resistivity ratio of clean Airco wire is slightly less than 50, so the termination copper has an estimated RRR in the range 25-50.⁷ (An RRR test in liquid hydrogen of a small section of termination would quickly resolve this uncertainty.)

In addition to surface resistivity and resistivity ratio, the quality of metallurgical bonding inside the termination affects overall lap joint resistance. In the swaging operation, the cable was hammered to remove voids and produce cold welds between adjacent strands. However, swaging does not produce a completely monolithic termination, and imperfect bonding between adjacent strands increases the resistance of the termination.³

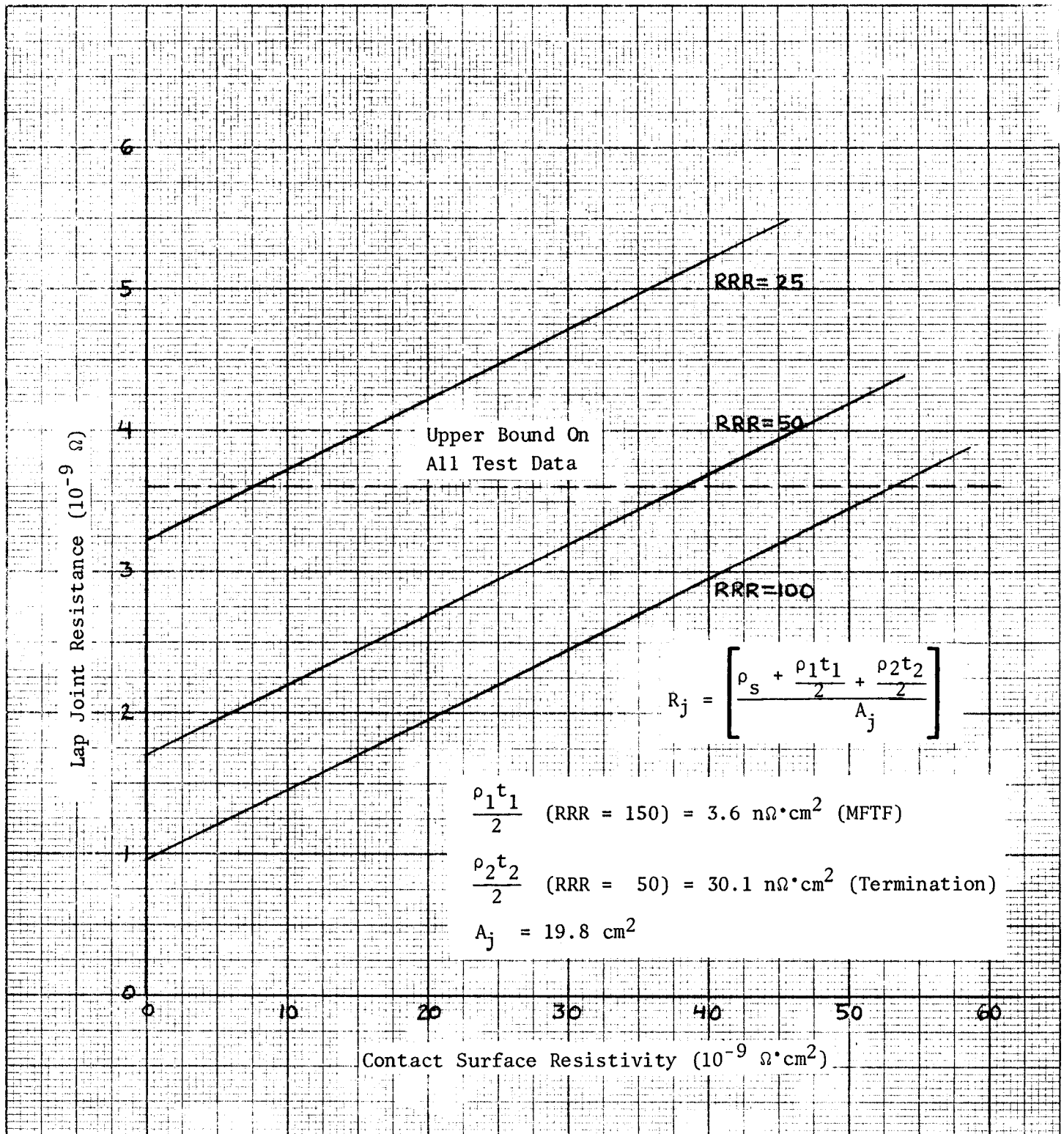


Figure 12. Lap joint resistance as a function of contact surface resistivity, with termination copper resistivity ratio as a parameter. The upper bound on all test data is $3.6 \text{ n}\Omega$. The formula for joint resistance shows that current transfer resistance $\left(\frac{\rho_1 t_1 + \rho_2 t_2}{2A_j} \right)$ is comparable to solder layer resistance $\left(\frac{\rho_s}{A_j} \right)$ at high currents.

With the apparent RRR of the termination copper 50 or less, an upper bound on solder layer surface resistivity is $40 \text{ n}\Omega \cdot \text{cm}^2$. It is interesting to note that the product of bulk copper resistivity and termination half thickness is closer than a factor of two to this number. Usually surface resistivity is significantly larger than the bulk resistivity-half thickness product, and surface resistivity determines the resistive behavior of the joint. For the termination lap joint experiment, however, this was not the case. At high currents, the current transfer term influenced the behavior of the lap joints. This is because at high currents longitudinal resistance due to filament saturation increased current transfer resistance. The resistivity-half thickness product at RRR's of 50 and 25 is shown below. These numbers should be compared to $40 \text{ n}\Omega \cdot \text{cm}^2$.

$$\frac{\rho t}{2} \text{ (termination RRR} = 50) = 30.1 \text{ n}\Omega \cdot \text{cm}^2$$

$$\frac{\rho t}{2} \text{ (termination RRR} = 25) = 60.2 \text{ n}\Omega \cdot \text{cm}^2$$

8.2 Longitudinal Resistance Model

The distribution of current within the lapped conductors of a joint is likely to be nonuniform, with some superconductive filaments carrying more current than others. The filaments closest to the joint will begin to saturate at low current, develop longitudinal resistance, and thereby produce a transverse flow of current to unsaturated filaments. In the case of an ICCS termination, one can think of strands that saturate and produce a transverse current flow to other strands. The longitudinal resistance decreases with increasing distance from the joint and finally disappears altogether as the current distribution evens out to the point at which no filaments are saturated.

(The characteristic distance associated with the disappearance of longitudinal resistivity is the current transfer length.) The purpose of considering longitudinal resistance as a discrete component of joint resistance is to offer a model for the apparent behavior of the "praying hands" lap joint at zero field and 12 kA (See Figure 8).

A grossly simplified model of a lap joint with provisions for longitudinal resistance is shown in Figure 13 below.

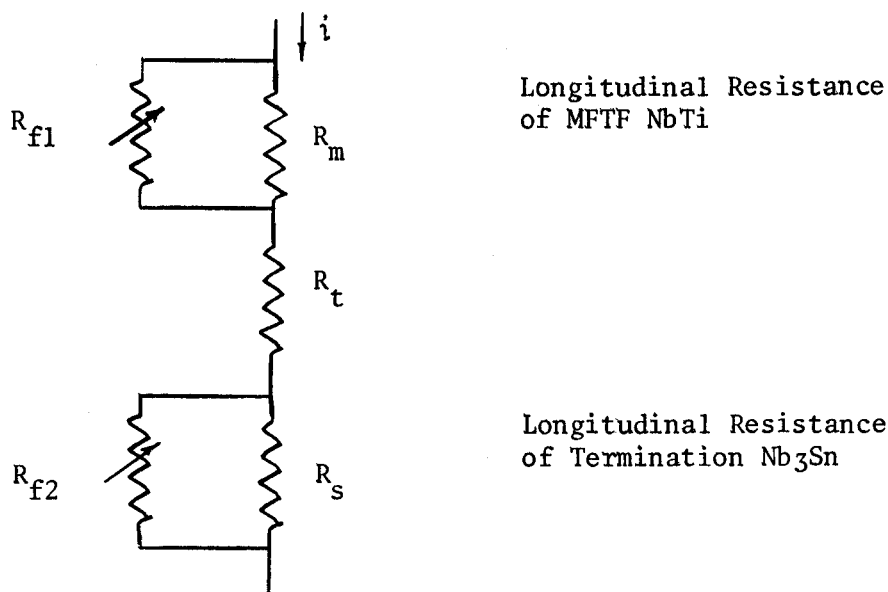


Figure 13. Lap joint model with discrete longitudinal resistance. The superconductors are modeled as variable resistors in parallel with normally conducting matrices.

Here R_t models the interface and all current transfer resistance associated with transverse current flow. R_m models the MFTF conductor core matrix resistance, and R_s models the termination stabilizer resistance. Filament resistances are modeled by R_{f1} and R_{f2} . The entire joint resistance then follows as

$$R_j = \frac{R_m R_{f1}}{R_m + R_{f1}} + R_t + \frac{R_s R_{f2}}{R_s + R_{f2}} \quad (10)$$

Superconductor resistivity can be modeled by

$$\rho = \rho_o (i/i_o)^{m-1} \quad (11)$$

where ρ_o is a reference resistivity corresponding to current i_o and m is an integer.¹² Equation 11 motivates an expression for superconductor resistance as

$$R = R_o (i/i_o)^{m-1} \quad (12)$$

where R_o is a reference resistance corresponding to current i_o . By choosing R_o equal to the resistance of the shunting copper, the longitudinal terms of (10) can be written as

$$\text{Longitudinal Resistance} = \frac{R_{cu}}{(i_o/i)^{m-1} + 1} \quad (13)$$

Assuming one of the two lapped conductors develops longitudinal resistance before the other, joint resistance can be approximated by

$$R_j = R_t + \frac{R_{cu}}{(i_o/i)^{m-1} + 1} \quad (14)$$

This model was applied to the volt-ampere data of the "praying hands" lap joint of Figure 8.

9. DISCUSSION

9.1 Cable Critical Current

From Figure 11, the critical current of the bare test cable at 12 T corresponds to 59% of its single wire expectation. The obvious question is why the unsheathed, bare cable did not act like 324 single wires in parallel? In fact, it acted more like 224 wires in parallel, with 100 wires missing.

At 12 tesla and 13.6 kA, the stable voltage drop across the cable was 120 μ V (voltage taps 9 and 10 in Figure 6). This voltage drop was over a length of approximately 8.7 cm (the centerline-to-centerline distance between legs of the hairpin). Hence, the average electric field along at least one of the parallel strands was 14 μ V/cm.

In single wire tests at MIT, hairpin voltage taps are spaced approximately 2.5 cm apart. Multiplying the average cable electric field by this spacing yields a voltage of $2.5 \times 14 = 34$ μ V, well above the 4 μ V normally used to define single wire critical current. The implication here is that some cable strands were prematurely current sharing, a result of an uneven current distribution in the cable.

Current sharing at 59% of expectation implies an uneven distribution of current among the 324 available Nb₃Sn strands. One explanation for this imbalance of current is lap joint design, because some of the available strands were buried deep inside the termination and did not reach the lap

joint surface. Another explanation is mechanical damage to the superconductor during compaction of the termination. A third, though less likely explanation, is mechanical damage to the cable after activation of the Nb₃Sn. A program is currently underway at MIT to quantify some of the parameters affecting the current carrying capacity of Nb₃Sn ICCS.

9.2 Background Noise

The test data were embedded in background noise consisting of a very low frequency sine wave (~ 0.01 Hertz), of unknown origin. The frequency of the sine wave appeared to change slightly, perhaps by ± 0.001 Hz, over a typical 200 second interval. The sine wave was evident with both zero magnetic field and zero hairpin current, and was also evident with nonzero magnetic field and nonzero hairpin current. An investigation of the instrumentation revealed no obvious internal signal source, and it is noteworthy that the two Biomation Waveform Recorders detected the same signal while essentially uncoupled (the recorders were coupled for simultaneous sweep triggering only).

The method of signal extraction was to measure lap joint voltages at constant hairpin current when the background sine wave passed through zero. Voltages measured by this technique were resistive in origin.

There was also evidence of baseline drift in the voltage readings; zero voltage at the beginning of a measurement did not necessarily correspond to zero voltage at the end of a measurement. Typical runs were from 100 to 300 seconds, times long enough for baseline drift to become significant (see Figure 7). The source of the baseline drift is also unknown.

The stated uncertainty in lap joint voltage measurements is $\pm 20 \mu\text{V}$ (See Figures 8-10). As explained above, the source of this uncertainty was the combination of very low frequency noise and baseline drift. To counteract these difficulties, it is recommended that in future experiments, long duration sweeps (at least 500 seconds) be made at zero field and zero current to quantify background noise and drift. When actual runs are made, it is recommended that 100 second initial and final voltage baselines be established. This is important since baseline drift could be as much as $20 \mu\text{V}$ in a five minute interval.

9.3 Recommendations for Future Work

Since the current distribution in the cable appeared to be nonuniform, the experiment should be repeated a second time with additional NbTi ribbons, one ribbon per joint, as jumpers between the nonlapped surfaces. Each ribbon would be u-shaped with the legs of the u running parallel to the lapped conductors. The presence of each ribbon would significantly increase the joint surface contact area, although the current path through either ribbon includes two solder layers rather than one. Jumpers should distribute current more evenly in the cable, resulting in lower lap joint losses and higher critical currents.

Another way to improve the cable current distribution would be to increase solder surface contact areas by increasing lap joint lengths by 50% from their present 15 cm (6") to 23 cm (9"), the total axial length of the short termination. This action would follow the original termination test plan where length (implicitly contact area) was considered a principal parameter. It is recommended that the experiment be repeated a third time using

23 cm joints. The prime motivation for this endeavor would be a better understanding of the relationship of critical current to lap joint contact area, recognizing that 23 cm lap joints may be too long for use in the 12 Tesla Coil (See Figure 1).

Since the field at the terminations was no greater than 500 gauss throughout the experiment, it is recommended that another experiment, with smaller termination lap joints, be built and tested in fields up to 5 tesla.

Since the resistivity ratio of the terminations is unclear, an activated 27 strand ICCS, compacted to 5% void, should be tested for RRR along with identical but uncompacted single wire samples. The single wire samples would serve as a control in this experiment.

Since no comprehensive study of ICCS lap joints has been attempted, it is recommended that one be made relating joint resistance to parameters such as cable twist pitch, termination compaction, solder joint contact area, solder thickness, and solder composition.

Since the internal condition of the termination is unknown, it is recommended that photomicrographs of sections of the two terminations be made. This would allow for evaluation of both the internal metallurgical bonding and the mechanical state of the Nb_3Sn .

9.4 Significance of Experiment

The experiment has proven that the 15 cm termination lap joints envisioned for the 12 Tesla Coil are thermally stable up to 21 kA. The results imply that the worst case heat load on the HFTF cryostat will be no more than 7 watts at 21 kA. In essence, this experiment legitimizes the lap joint concept described in the text.

10. ACKNOWLEDGMENT

We wish to acknowledge the precise and thorough work of Cris Cyders, who helped in the design and execution of the experiment. His efforts made the experiment possible.

11. NOMENCLATURE

A_j (cm^2)	Lap joint contact surface area
i (A)	Current
i_o (A)	Reference current
m (-)	Positive integer
R_{cu} (Ω)	Copper resistance
R_{f1} (Ω)	Filament resistance, superconductor 1
R_{f2} (Ω)	Filament resistance, superconductor 2
R_j (Ω)	Lap joint resistance
R_m (Ω)	Matrix resistance
R_o (Ω)	Reference resistance corresponding to i_o
R_s (Ω)	Stabilizer resistance
R_t (Ω)	Transverse component of lap joint resistance
t (cm)	Conductor thickness
t_1 (cm)	Thickness, conductor 1
t_2 (cm)	Thickness, conductor 2
v_i (v)	Voltage at tap i

ρ ($\Omega \cdot \text{cm}$)	Resistivity
ρ_1 ($\Omega \cdot \text{cm}$)	Resistivity, conductor 1
ρ_2 ($\Omega \cdot \text{cm}$)	Resistivity, conductor 2
ρ_m ($\Omega \cdot \text{cm}$)	Matrix resistivity
ρ_o ($\Omega \cdot \text{cm}$)	Reference resistivity corresponding to i_o
ρ_s ($\Omega \cdot \text{cm}^2$)	Surface resistivity

12. REFERENCES

1. Hoenig, M.O., et. al., "Cryogenic Aspects of the Internally Cooled, Cabled Superconductor (ICCS) for the 12 Tesla Program," Advances in Cryogenic Engineering, Vol. 27, 1982.
2. Hoenig, M.O., et. al., "Progress in the ICCS-HFTF 12 Tesla Coil Program," IEEE Trans. MAG-17, No. 1, Jan. 1981, p. 638.
3. Waldman, S.J., et. al., "Monolithic Terminations for Multistrand NbTi and Nb₃Sn Cables," Advances in Cryogenic Engineering, Vol. 26, 1980, p. 608.
4. Sanger, P.A., et. al., "Critical Properties of Multifilamentary Nb₃Sn Between 8 and 14 Tesla," IEEE Trans. MAG-17, No. 1, Jan. 1981, p. 666.
5. Blaugher, R.D., et. al., "Experimental Test and Evaluation of the Nb₃Sn Joint and Header Region for the Westinghouse LCP Coil," IEEE Trans. MAG-17, No. 1, Jan. 1981, p. 467.
6. Westinghouse Electric Corporation, "Large Coil Program-Manufacturing Plan," Phase 2 Final Report to Union Carbide Corp., Vol. IV, March 31, 1980, p. 31.
7. Montgomery, A.G., Unpublished RRR Test Data, MIT, 1981.
8. Westinghouse Electric Corporation, "Large Coil Program-Introduction," Phase 2 Final Report to Union Carbide Corp., Vol. I, March 31, 1980, p. 223.
9. Hoenig, M.O., "Internally Cooled Cabled Superconductors," Cryogenics, July 1980, p. 373.
10. Deis, D.W., et. al., "Fabrication of the MFTF Magnet Windings," IEEE Trans. MAG-15, No. 1, Jan. 1979, p. 534.
11. Goodrich, L.F., et. al., "Lap Joint Resistance and Intrinsic Critical Current Measurements on a NbTi Superconducting Wire," IEEE Trans. MAG-17, No. 1, Jan. 1981, p. 69.
12. Steeves, M.M., Unpublished Short Sample Test Data, MIT, 1981-82.
13. Dresner, L., "Distribution of Current Among the Filaments of a Multifilamentary Superconductor Close to Input Leads," Cryogenics, May 1978, p. 285.
14. Hatch, A.M., et. al., "The Resistance of Soldered Joints in Superconducting Magnet Windings," Avco Everett Research Laboratory, July 1975.

15. Rackov, P.M., et. al., "Superconductor Joining Methods for Large CTR Magnets," Sixth Symposium on Engineering Problems of Fusion Research, Nov. 1975, p. 593.

PLASMA FUSION CENTER INTERNAL DISTRIBUTION:

PFC BASE MAILING LIST

Argonne National Laboratory, TIS, Reports Section
Associazione EURATOM - CNEN Fusione, Italy, The Librarian
Battelle-Pacific Northwest Laboratory, Technical Info Center
Brookhaven National Laboratory, Research Library
Central Research Institute for Physics, Hungary, Preprint Library
Chinese Academy of Sciences, China, The Library
The Flinders University of S.A., Australia, Jones, Prof. I.R.
General Atomic Co., Library
General Atomic Co., Overskei, Dr. D.
International Atomic Energy Agency, Austria,
Israel Atomic Energy Commission, Soreq Nucl. Res. Ctr., Israel
Kernforschungsanlage Julich, FRG, Zentralbibliothek
Kyushu University, Japan, Library
Lawrence Berkeley Laboratory, Library
Lawrence Livermore Laboratory, Technical Info Center
Max-Planck-Institut fur Plasma Physik, FRG, Main Library
Nagoya University, Institute of Plasma Physics, Japan
Oak Ridge National Laboratory, Fusion Energy Div. Library
Oak Ridge National Laboratory, Derby, Roger
Physical Research Laboratory, India, Sen, Dr. Abhijit
Princeton University, PPL Library
Rensselaer Polytechnic Institute, Plasma Dynamics Lab.
South African Atomic Energy Board, S. Africa, Hayzen, Dr. A.
UKAEA, Culham Laboratory, England, Librarian
US Department of Energy, DOE Library
Universite de Montreal, Lab. de Physique des Plasmas, Canada
University of Innsbruck, Inst. of Theoretical Physics, Austria
University of Saskatchewan, Plasma Physics Lab., Canada
University of Sydney, Wills Plasma Physics Dept., Australia
University of Texas at Austin, Fusion Res. Ctr., Library
University of Wisconsin, Nucl. Eng. Dept., UW Fusion Library

INTERNAL MAILINGS

MIT Libraries

Industrial Liaison Office

G. Bekefi, A. Bers, D. Cohn, B. Coppi, R.C. Davidson,
T. Dupree, S. Foner, J. Freidberg, M.O. Hoernig, M. Kazimi,
L. Lidsky, E. Marinar, J. McCune, J. Meyer, D.B. Montgomery,
J. Moses, D. Pappas, R.R. Parker, N.T. Pierce, P. Politzer,
M. Porkolab, R. Post, H. Pradaude, D. Rose, J.C. Rose,
R.M. Rose, B.B. Schwartz, L.D. Smullin, R. Temkin, P. Wolff,
T-F. Yang